Harmful Algae 129 (2023) 102517

Contents lists available at ScienceDirect

Harmful Algae

journal homepage: www.elsevier.com/locate/hal

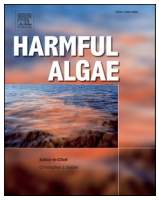

Original Article

Operational modelling to assess advective harmful algal bloom development and its potential to impact aquaculture

Paul Dees [a,b,*], Andrew Dale [a], Callum Whyte [a], Beth Mouat [c], Keith Davidson [a]

[a] Scottish Association for Marine Science, Oban, Argyll, PA37 1QA, United Kingdom
[b] Geophysical Institute, University of Bergen, 5020 Bergen, Norway
[c] UHI Shetland, Port Arthur, Scalloway ZE1 0UN, United Kingdom

ARTICLE INFO

Edited by Dr. C. Gobler

Keywords:
HABs
Dinophysis
DSP
Aquaculture
AMM15
Modelling

ABSTRACT

A particle tracking model is described and used to explore the role of advection as the source of harmful algal blooms that impact the Shetland Islands, where much of Scotland's aquaculture is located. The movement of particles, representing algal cells, was modelled using surface velocities obtained from the 1.5 km resolution Atlantic Margin Model AMM15. Following validation of model performance against drifter tracks, the model results recreate previously hypothesised onshore advection of harmful algal cells from west of the archipelago during 2006 and 2013, when exceptional *Dinophysis* spp. abundances were measured at Shetland aquaculture sites. Higher eastward advection of *Dinophysis* spp. cells was also suggested during 2018. Wind roses explain this higher eastward advection during 2006, 2013 and 2018. The study suggests that the European Slope Current is important for the transport of harmful algal blooms, particularly those composed of dinoflagellates.

1. Introduction

Harmful algal blooms (HABs) are a frequent disruption to shellfish aquaculture worldwide (Berdalet et al., 2016), including around the coasts of Scotland (Bresnan et al., 2021; Gianella et al., 2021; Martino et al., 2020). Within Scotland, HABs are a particular threat in and around the Shetland Islands, where approximately 80 % of the UK's *Mytilus edulis* are farmed and harvested (Martino et al., 2020).

The majority of HAB species are dinoflagellates (Bresnan et al., 2021; Hinder et al., 2012), and frontal regions are thought to influence the distribution and formation of their blooms (Raine et al., 2017). In particular, diarrhetic shellfish poisoning (DSP)-causing *Dinophysis* spp. has been measured at a higher abundance in the proximity of fronts (Franks, 1992a; Franks and Walstad, 1997; Paterson et al., 2017; Siemering et al., 2016) and fronts have been implicated as sites of bloom initiation (Franks, 1992b). A stable front, however, is also an impediment to advection of HABs (Franks, 1992b; Paterson et al., 2017). Confusion about how frontal regions influence HAB formation and advection means the importance of frontal regions west of the Shetland Islands is not yet fully understood. It has, however, been hypothesised that HABs are generated at or near fronts (Raine et al., 2017) and subsequently advected to the coastline by eastward currents (Raine et al., 2017; Whyte et al., 2014). It has also been hypothesised that dinoflagellate dominated HABs composed of *K. mikimotoi* or *Dinophysis* spp. can be transported northwards in the European Slope Current (ESC), a persistent poleward flow at the NW European shelf edge (illustrated in Fig. 1) (Gillibrand et al., 2016), and subsequently advected from the shelf edge to the Scottish mainland or to Shetland (Gillibrand et al., 2016; Whyte et al., 2014). Any attempt to improve the prediction of HABs in complex waters must take frontal regions and water movement into account.

Because advective transport has been shown to influence HAB initiation and movement, particle tracking models have been used to hindcast significant HAB events. Using this methodology, possible pathways of a large *Alexandrium fundyense* bloom in the Gulf of Maine during 2006 were faithfully hindcast by a numerical model (Li et al., 2009). In the Pacific Northwest, another numerical model has been used to hindcast pathways of *Pseudo-nitzschia* spp. to the coast, made challenging by the complex coastline and the riverine plume of the Columbia River (Giddings et al., 2014). Along the Iberian coast, a particle tracking model using PCOMS (Mateus et al., 2012) has been used to predict potential pathways of dinoflagellates and diatoms to the coast (Pinto et al., 2016). Such models are highly useful but require observational data and validation to ensure their accuracy.

* Corresponding author.
E-mail address: paul.dees@uib.no (P. Dees).

https://doi.org/10.1016/j.hal.2023.102517
Received 27 June 2023; Received in revised form 5 September 2023; Accepted 22 September 2023
Available online 29 September 2023

Lagrangian models such as these are typically validated by comparisons to data from remote sensing and cell counts of potential harmful algae at the coast (Mateus et al., 2019, 2012; Pinto et al., 2016), or to high spatial resolution CTD moorings (Giddings et al., 2014; Li et al., 2009). Several European projects are, or have been, concerned with understanding and predicting such advective HAB events, including "ASIMUTH" and "PRIMROSE". These projects have identified three data sources needed for an effective HAB early warning system (EWS): satellite imagery, *in situ* data and numerical tools (Davidson et al., 2016; Maguire et al., 2016; Mateus et al., 2019). A relevant particle tracking model is one that can provide useful information to aquaculture stakeholders and managers not available through other means, and whose accuracy can be verified using observational data (Pinto et al., 2016).

In Scottish waters, some success has been found combining these data sources to track HAB events. For example, Gillibrand et al. (2016) used a POLCOMS model-based analysis to demonstrate that the exceptional 2006 bloom of potentially fish-killing *Karenia mikimotoi* progressed around the Scottish coast at a rate that could not be explained simply by transport on the coastal current, suggesting that the shelf edge current was important in cell transport. Aleynik et al. (2016) subsequently demonstrated the use of an unstructured grid model based on the Finite Volume Community Ocean Model (FVCOM) (Chen et al., 2011) to simulate HAB events in Scottish waters, with Davidson et al. (2021) using this "WeStCOMS" model to generate HAB forecasts within an operational EWS (www.HABreports.org). The large proportion of shellfish aquaculture taking place on Shetland, together with the economic damage and health concerns resulting from advected HABs (Martino et al., 2020; Whyte et al., 2014), mean an EWS for use in Shetland is beneficial.

Following nearshore validation, our study used surface currents modelled by AMM15 to underpin a particle tracking model which was used to determine the transport and development of HABs. This model was also used to test whether algal blooms impacting coastal aquaculture sites on the Shetland coast frequently originate from the same geographical areas on the shelf. The model thus has the potential to allow the development of a targeted "smart" offshore HAB early warning monitoring effort, perhaps by remote sensing or by moored instrumentation. The model can provide HAB forecasts fit for the 21st Century to aquaculture stakeholders and other interested parties.

2. Methods

The area of focus for the particle tracking model is bounded by 59° and 62.74° North, and −8° and 2.5° East (Fig. 1), including the north of the Orkney Islands, the seas surrounding Shetland, part of the Atlantic Ocean west of Shetland, and the adjoining shelf edge. The methods section is summarized by a flowchart detailing the research process (Supplementary 1).

2.1. Harmful bloom simulation using particle tracking within AMM15

Hourly surface velocities for the years 2006 – 2013 and 2016 from a configuration run of the AMM15 hydrodynamic model (Graham et al., 2018) were acquired directly from the model authors. The contiguous period between 2006 and 2013 has been studied elsewhere because of large *Dinophysis* spp. blooms (Whyte et al., 2014), so obtaining these data was prioritised. Data from years 2014 and 2015 could not be accessed and were excluded from analysis, but as *Dinophysis* spp. abundance from these years was not exceptionally high (Fig. 2) this was not considered problematic. Data from 2017 to 2018 were obtained from the operational model, as the data product NORTHWEST-SHELF_ANALYSIS_FORECAST_PHY_004_013 via the Copernicus Marine Service. Use of the configuration run allowed evaluation of HAB dynamics in a greater number of years than the operational model alone would allow. It should be noted, however, that these earlier runs did not undergo the same operational forcing and boundary parameters as the validated model from after 2016.

In each model simulation for years 2006 – 2013, 7778 particles were distributed evenly throughout the model domain, trapped at the ocean surface. During 2016 – 2018, 7896 particles were used for each model simulation and the model was extended to 3° E. Surface currents acted on the particles by using interpolated velocities to calculate successive positions of each particle:

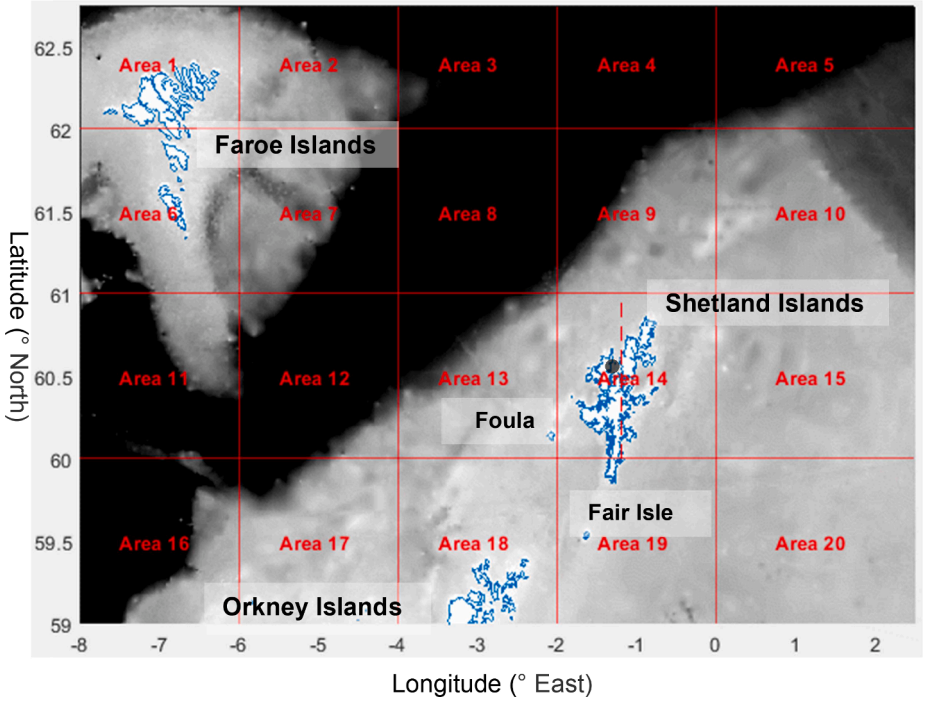

Fig. 1. Map of the study area. Bathymetry and coastline data from Digimap®. Black corresponds to depths greater than 500 m. Scatsta Airport has been marked with a black circle (●). The study area has been divided into areas which will be described in Section 2.2.

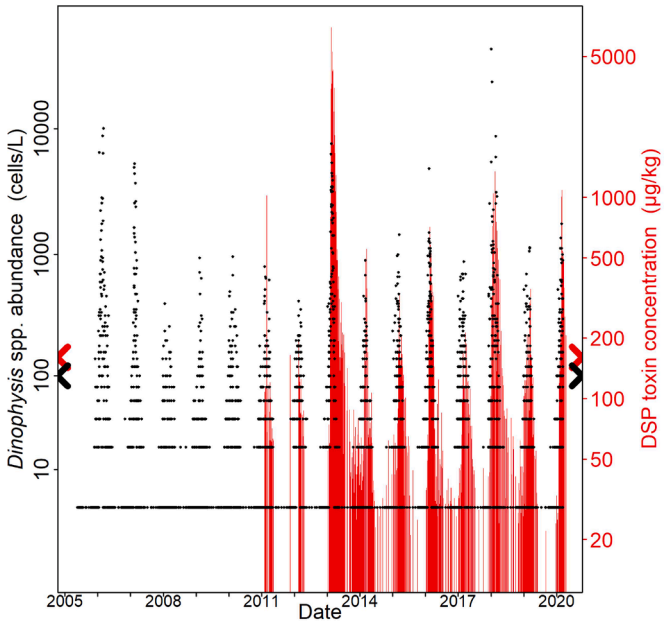

Fig. 2. Time series graphs showing the abundance of *Dinophysis* spp. determined by monitoring in black points, with the black markers (<, >) indicating the threshold abundance limit of *Dinophysis* spp. in the water column (100 cells L^{-1}). Abundance data have been transformed using $\log_{10}(x + y)$, where x = abundance and y = half the minimum non-zero abundance. The concentration of OA, DTXs, and PTXs in homogenized mussel flesh (µg/kg) is shown by vertical red lines, and red markers (<, >) showing the regulatory limit of DSP concentration in shellfish (160 µg kg^{-1} OA equivalents). Toxin data were transformed using log(x), where x is the concentration of toxins in mussel flesh.

$$(X_{T+\Delta T}, Y_{T+\Delta T}) = (X_T, Y_T) + (U_T, V_T)\Delta T + (R_1, R_2)\sqrt{2k_H \Delta T} \quad (1)$$

where (X_T, Y_T) is the position of the particle at time T, the time step is ΔT (here one hour), and (U_T, V_T) is the 2-dimensional advection velocity obtained from AMM15. The final term is a random diffusion representing unresolved influences (R_1 and R_2 are randomly −1 or +1). The horizontal diffusion coefficient k_H was assigned the constant value of 0.25 m^2 s^{-1}. Reproduction of plankton populations or zooplankton predation were not modelled, and each model run was limited to four weeks.

Model simulations were initiated from the first or second week of May until the second or third week of August in each year. Simulations began on Sunday, and successive simulations were started seven days after the starting date of the previous simulation. Results from the same twelve weeks per year were analysed, and in some years earlier and later weeks were also saved depending on how early Sunday was in the particular year. Simulations from each starting date throughout the study period were rerun 24 times using different randomly generated dispersion to allow statistical comparisons between areas (Fig. 1). The percentage of particles which landed on Shetland from specific regions of the study area were then evaluated and compared.

Particles were permitted to move anywhere in the surface of the study area. When any particle reached the boundaries of the model domain or approached land, it was stopped and its location recorded. A distinction was made between particles that landed on Shetland excluding Fair Isle (where no aquaculture is located), and those that landed on other land masses (see Fig. 1). The location of particles was allowed to change every hour depending on surface currents. To evaluate the origin of cells that impacted aquaculture areas, the starting locations of particles which landed on Shetland were recorded.

In the results presented here we focus on 2006, 2007, 2013 and 2018, as the abundance of *Dinophysis* spp. in the region exceeded 5000 cells L^{-1} at least once during those years (Fig. 2). Aside from these blooms, shellfish toxin concentration exceeded the regulatory limit of 160 µg kg^{-1} OA equivalents even when cell abundance was less than the regulatory threshold of 100 cells L^{-1} (Fig. 2). The mouse bioassay was used before 2011, meaning that toxicity of shellfish could not be quantified before this date (Fig. 2).

To determine whether there were distinct regions of bloom initiation around Shetland, the study area was divided into twenty rectangles along degrees of latitude and every two degrees of longitude (Fig. 1). As Area 14 included all of Shetland, it was divided along the approximate length of Shetland at −1.185° longitude to allow discrimination between east and west coasts in our analyses (Fig. 1). These two areas were called Area 14 W and 14E (Fig. 1).

The total number of particles initiating in each of area displayed in Fig. 1 that landed on the coast of Shetland were enumerated. The percentage of all the particles which started in each region that made landfall on Shetland was then calculated. The movement of particles was partly determined by the random diffusive effect from Eq. (1), meaning the end point of particles in each model simulation differed. Repeating each model simulation 24 times allowed a sufficiently large sample size to draw conclusions about the differences between mean percentages of particles from each area which landed on the coast of Shetland.

2.2. Model validation: drifter deployment west of Shetland

To determine how well AMM15 models the speed and direction of surface currents west of Shetland, drifters were deployed on two occasions during 2018. On 30th May 2018, three SouthTEK Offshore Nomad drifters were deployed. A second group of four similar drifters were deployed on 4th July 2018. Two of the second group of drifters were equipped with solar panels to prolong their transmission time. SouthTEK drifters were chosen because they have successfully been used in a number of other studies including to assist with oil spill forecasting in Italian seas (Ribotti et al., 2018) and clarifying surface currents in the Gibraltar Strait (Bolado-Penagos et al., 2017). Coverage of the GPRS mobile telephone network is poor around Shetland. Drifters were therefore equipped with Iridium capability, which allowed transmission of their positions without interruption. Drifters were drogued at a depth of 10 m.

Particle tracking model simulations to compare to drifters were initiated at the same time and location as drifter deployments. This was done by distributing particles over a 21 × 21 grid covering an approximate 1.2 km^2 area from where each drifter began reporting. The separation between particles was approximately 50 m, far less than the 1.5 km horizontal resolution of the AMM15 model. Particle tracking model simulations matched the length of drifter deployments: 473 h from late May 2018 until mid-June 2018, and 132 h during July 2018. To discern how much the random dispersal effect from Eq. (1) affected the pathways of modelled particles, modelled simulations were repeated 50 times.

2.3. Wind

Hourly wind speeds were obtained from the Met Office recording station at Scatsta Airport (Fig. 1). Data were downloaded from the Centre for Environmental Data Analysis (www.ceda.ac.uk). Wind roses were constructed for the period between the beginning of May and the end of August using the R package “windrose” (Hopper, 2014).

2.4. Chlorophyll data

High resolution chlorophyll concentration in surface waters was obtained from ACRI-ST Company as part of Copernicus Marine Environment Monitoring Service (Le Traon et al., 2015). Surface concentration of chlorophyll-a and phaeophytin (hereafter referred to as chlorophyll) was calculated by applying algorithms to the merged product of the following satellite ocean colour sensors: SeaWIFS, MODIS

Aqua, MODIS Terra, MERIS, VIIRS NPP, VIIRS-JPSS1, OLCI-S3A and S3B. In the current study area, which included mainly coastal seas, the OC3-OC4 algorithms and OC5 algorithms were more suitable (Le Traon et al., 2015; O'Reilly et al., 1998), in comparison to earlier chlorophyll estimation algorithms designed for oligotrophic water bodies (Hu et al., 2012). The final chlorophyll product returns concentrations in surface waters at 1 km resolution over the study area.

L4 data, which are chlorophyll estimates which have not undergone interpolation in areas obscured by clouds, were used in this study. The global L4 chlorophyll product is strongly correlated to *in situ* chlorophyll measurements, returning an r^2 value of 0.71 (Garnesson et al., 2021). Copernicus assigns error values to individual chlorophyll estimates. To minimize the probability of incorporating less than accurate chlorophyll estimates in this study, values associated with an error value of 50 % or more were discarded from analysis.

Surface chlorophyll concentrations were extracted for the area confined by 56° and 62° N, and −9° and 3° E. A larger area was chosen to display surface chlorophyll data, in comparison to particle tracking models, to show the effect of large-scale oceanographic features on chlorophyll. Using a larger area also allowed for a wider view, which was helpful to observe chlorophyll moving northwards from locations outside the study area.

3. Results

3.1. Comparison between drifter deployments and AMM15 currents

The tracks and end points of particles advected by AMM15 surface currents were compared to drifter movements (Fig. 3). During the drifter deployment of 30th May 2018, drifters were tracked first moving offshore westwards and south westwards (Dees, 2021a; Fig. 3A). Towards the end of the deployment, drifters were tracked moving towards the Shetland coastline and two of them landed to the South of St Magnus Bay (Dees, 2021a; Fig. 3A). Particle tracking model simulations show particles spreading out over a similar area compared to drifters (Fig. 3A). The drifter positions which overlapped with the least number of modelled particle positions were those West of Foula, which still showed agreement, and those close to the southwest Shetland coast (Fig. 3A).

Drifters deployed on 4th July 2018 moved southwest around the south of St Magnus Bay until they landed on the coast (Dees, 2021a; Fig. 3B). Modelled particles also moved towards Shetland coast during this period (Fig. 3B), and an approximately equal number of modelled particles moved around the north and south borders of St Magnus Bay (Dees, 2021a; Fig. 3B).

3.2. Particle tracking using AMM15 current velocities

Two animations for each model simulation were made, one showing particles moving under the influence of modelled currents in hourly increments (Table 1) and one showing whether particles had landed or were still moving (see Fig. 4 for details). In all simulations, the ESC can be inferred from its action on particles at the shelf edge (Figs. 4–7). The animations demonstrate that particles which began northwest of the continental shelf were propelled northwards by heightened current speeds in the ESC, compared to particles starting on the shelf (Table 1). Particles usually moved faster when between Orkney and Fair Isle than between Shetland and Fair Isle (Table 1), indicative of the Scottish Coastal Current (Hill et al., 1997). Eastward and westward movement of particles on the shelf had considerable inter- and intra-annual variation, but in all simulations particles in most of the study area indicated northwards advection by water currents (Table 1).

3.2.1. Particle tracking during 2006

In 2006, surface currents transported modelled particles, from as far away as the shelf edge west of Shetland to the coast (Fig. 5). During May, mid-June and early July, particles landing on the Shetland coastline originated from west of the shelf edge (Fig. 5A, C and D). Surface currents from early June and later in July 2006 were less likely to include transported particles from the shelf edge (Fig. 4B, E and F, in which the magenta dots do not extend to the shelf edge).

3.2.2. Particle tracking during 2007

Particles which landed on Shetland during 2007 did not originate from as distant from Shetland as during 2006, and none originated from the ESC (Fig. 5). Simulations beginning during June 2007 showed particles were more likely to be transported towards Shetland from the east, and hence were more likely to impact the east coast of Shetland (Fig. 5B and C, Table 1). In simulations beginning in early to mid-July, particles landing on Shetland originated from all around the perimeter of the

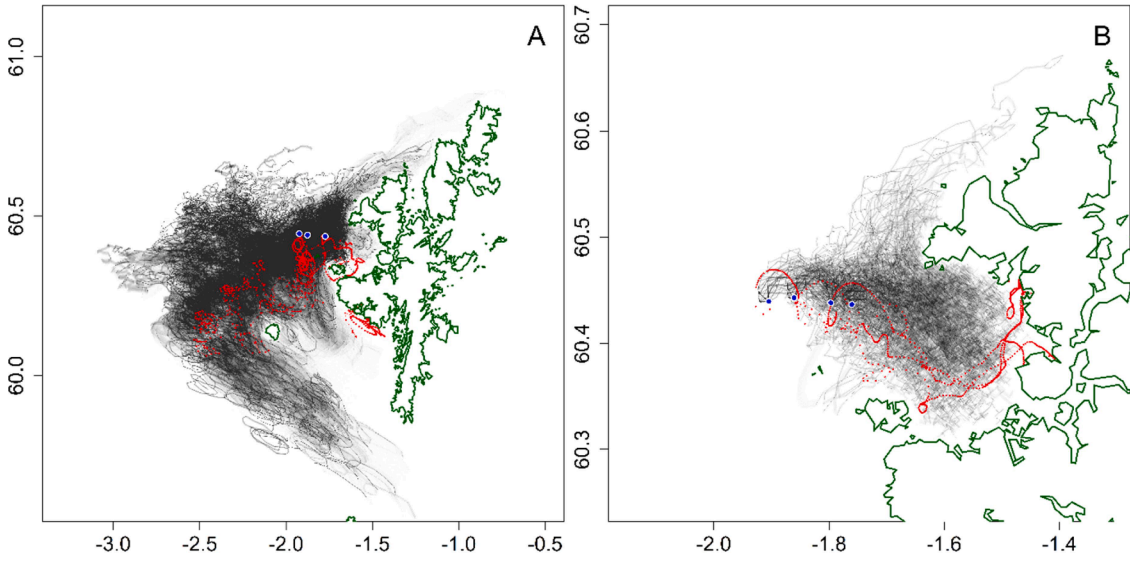

Fig. 3. Results of simulated particles operating under the influence of AMM15 using equations 1 in black, and drifter deployments in red. Modelled particles were plotted using translucent lines, allowing overlapping tracks to be identified; darker colours therefore indicate where there are more overlapping tracks. Particle tracking simulations were run from A 30th May until 19th June 2018, and B from 4th July until 10th July 2018. Each modelled drifter deployment was repeated 50 times. Blue points surrounded by white show the starting points of drifters and modelled particles.

Table 1
Links to animated gifs of the output of representative particle tracking model simulations for each week analysed, using mean hourly current velocity data from AMM15. Particle tracking simulations for years when exceptional blooms were not detected were also linked to in the bottom rows. The model domain was the area bounded by 59° and 62.74° N and −8° and 3° E. Models were run for 28 days.

Year	Start date	End date	Animations
2006	21/05/2006	18/06/2006	https://doi.org/10.6084/m9.figshare.16988503
	04/06/2006	02/07/2006	
	18/06/2006	16/07/2006	
	02/07/2006	30/07/2006	
	16/07/2006	13/08/2006	
	30/07/2006	27/08/2006	
2007	20/05/2007	17/06/2007	https://doi.org/10.6084/m9.figshare.16988815
	03/06/2007	01/07/2007	
	17/06/2007	15/07/2007	
	01/07/2007	29/07/2007	
	15/07/2007	12/08/2007	
	29/07/2007	26/08/2007	
2013	23/05/2013	21/06/2013	https://doi.org/10.6084/m9.figshare.16988986
	02/06/2013	30/06/2013	
	16/06/2013	14/07/2013	
	30/06/2013	28/07/2013	
	14/07/2013	12/08/2013	
	28/07/2013	26/08/2013	
2018	20/05/2018	28/06/2018	https://doi.org/10.6084/m9.figshare.16989034
	27/05/2018	25/06/2018	
	03/06/2018	01/07/2018	
	17/06/2018	15/07/2018	
	01/07/2018	29/07/2018	
	15/07/2018	13/08/2018	
	29/07/2018	27/08/2018	
	12/08/2018	10/08/2018	
2008, 2009, 2010, 2011, 2012, 2016, 2017			https://doi.org/10.6084/m9.figshare.16988920.v1 https://doi.org/10.6084/m9.figshare.16988923.v1 https://doi.org/10.6084/m9.figshare.16988932.v1 https://doi.org/10.6084/m9.figshare.16988938.v1 https://doi.org/10.6084/m9.figshare.16988968.v1 https://doi.org/10.6084/m9.figshare.16988992.v1 https://doi.org/10.6084/m9.figshare.16989025.v1

archipelago (Fig. 5D and E). For the simulation beginning at the end of July more particles landing on Shetland came from west of the islands (Fig. 5F).

3.2.3. Particle tracking during 2013

In the first weeks of the *Dinophysis* spp. growth season of 2013, most particles landing on Shetland do not appear to have come from further away than 30 km from the east and west coastlines of the archipelago (Fig. 6A). No modelled particles which landed on Shetland originated from near the ESC (Figs. 6A and 7B). From the beginning of June, the direction of currents appeared to change, and most particles landing on Shetland came from west of Shetland in all subsequent simulations (Fig. 6B–F). In simulations which started during June 2013, surface currents brought particles from as far away as between −7° and −8° East, to land on west Shetland, which included some particles directly from the ESC (Fig. 6C and D).

3.2.4. Particle tracking during 2018

Because the period of peak *Dinophysis* spp. abundance was earlier than other years, results from an extra model simulation have been included for 2018. Starting from 6th May 2018, most particles which landed on Shetland originated from southwest of the archipelago (Fig. 7A). In simulations starting at the end of May and beginning of June 2018, many particles landing on Shetland came from east of the islands (Fig. 7B and C). The presence of particles which were transported towards Shetland from southwest of the islands, in addition to particles from the east during the beginning of June, likely indicates currents shifting to predominantly eastward after mid-June (Fig. 7B and C). In later animations, which began after the beginning of June 2018, most particles came from west of Shetland (Fig. 7D–G).

3.2.5. Statistical comparison of particle tracking results

The number of modelled particles which landed on Shetland differed by region (see Fig. 1 and Section 2.1). As stated in Section 2.1, model simulations were run for 12 weeks per year, and the results of 24 simulations of each week were saved. The boxplot showing the percentages of particles which originated from the 21 specific subareas of the main study area which landed on Shetland shows the highest percentages came from Areas 9, 11 – 15 and 17 – 19, particularly Areas 13, 14W and 14E (Fig. 8). In contrast to the percentage of particles originating from other areas, the percentage of particles originating from Area 14W and 14E are always greater than zero (Fig. 8). This means of all particles which began in Areas 14W and 14E, at least some landed on Shetland in every simulation (Fig. 8). Particles which originated from Areas 1 – 8 and Area 20 almost never landed on Shetland (Fig. 8).

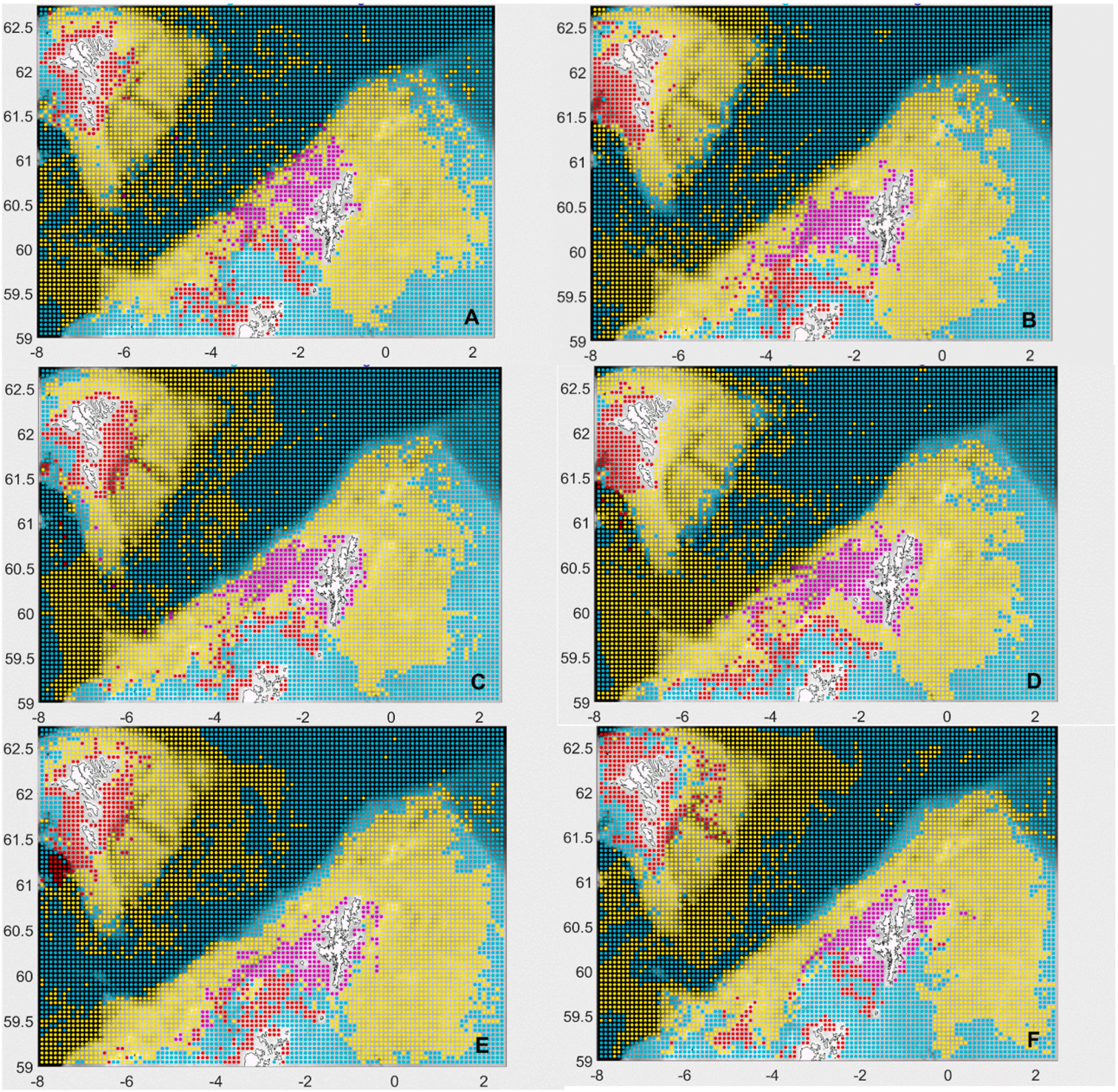

Fig. 4. Starting position of particles from tracking models which have been run over 28 days starting from A 21st May 2006, B 4th June 2006, C 18th June 2006, D 2nd July 2006, E 16th July 2006 and F 30th July 2006. Particles have been colour coded depending on where they were located after 28 days; yellow particles were still at sea, red particles landed on the Faroe or Orkney Islands or Fair Isle, magenta particles landed on Shetland (including Foula), and turquoise particles exceeded the boundaries of the map. Bathymetry has been marked using an underlying greyscale.

Area 14E was where the highest percentage of particles which landed on Shetland, and also where the greatest range in percentages of particles landing on Shetland, originated from (Fig. 8). Compared to Area 13 and 14E, there is little variance in the percentage of particles landing on Shetland coming from Area 14W (Fig. 8). Likely due to this lower variance, there were fewer significant differences between year groups for this region when assessed by ANOVA and pairwise t-tests ($p > 0.05$). For Area 13, however, the differences between year groups in mean percentages of particles that landed on Shetland in different years was significant at the 0.01 % level when assessed by ANOVA. Levene's Test (Levene, 1960) showed the assumption of equal homogeneity was violated ($p < 0.01$), so pairwise t-tests were used to show the percentage of particles during 2006 which originated from Area 13 was significantly higher than all other years ($p < 0.001$). The percentage of particles that landed on Shetland and originated from Area 13 during 2013 was significantly higher than all years, excluding 2006 ($p < 0.05$). Pairwise t-tests indicated that the mean percentage of particles originating from Area 13 during 2018 was significantly higher than other years apart from 2006, 2010 and 2013 ($p < 0.001$).

A visual inspection of these data indicated again that there are significant differences between years when using Area 13 as a reference point (Fig. 9). During 2006, the percentage of particles originating from Area 13 was significantly higher than other years for eight weeks during May and August (Fig. 9A). The percentage of particles originating from Area 13 during 2013 remained higher than other years for five weeks, and higher absolute percentages were measured (Fig. 9A). In contrast, the intra and interannual variation of percentages of particles originating from Area 14W which landed on Shetland are much smaller than Area 13 (Fig. 9). Pairwise t-tests indicated the percentages of particles originating from Area 14W during 2006 were significantly higher than

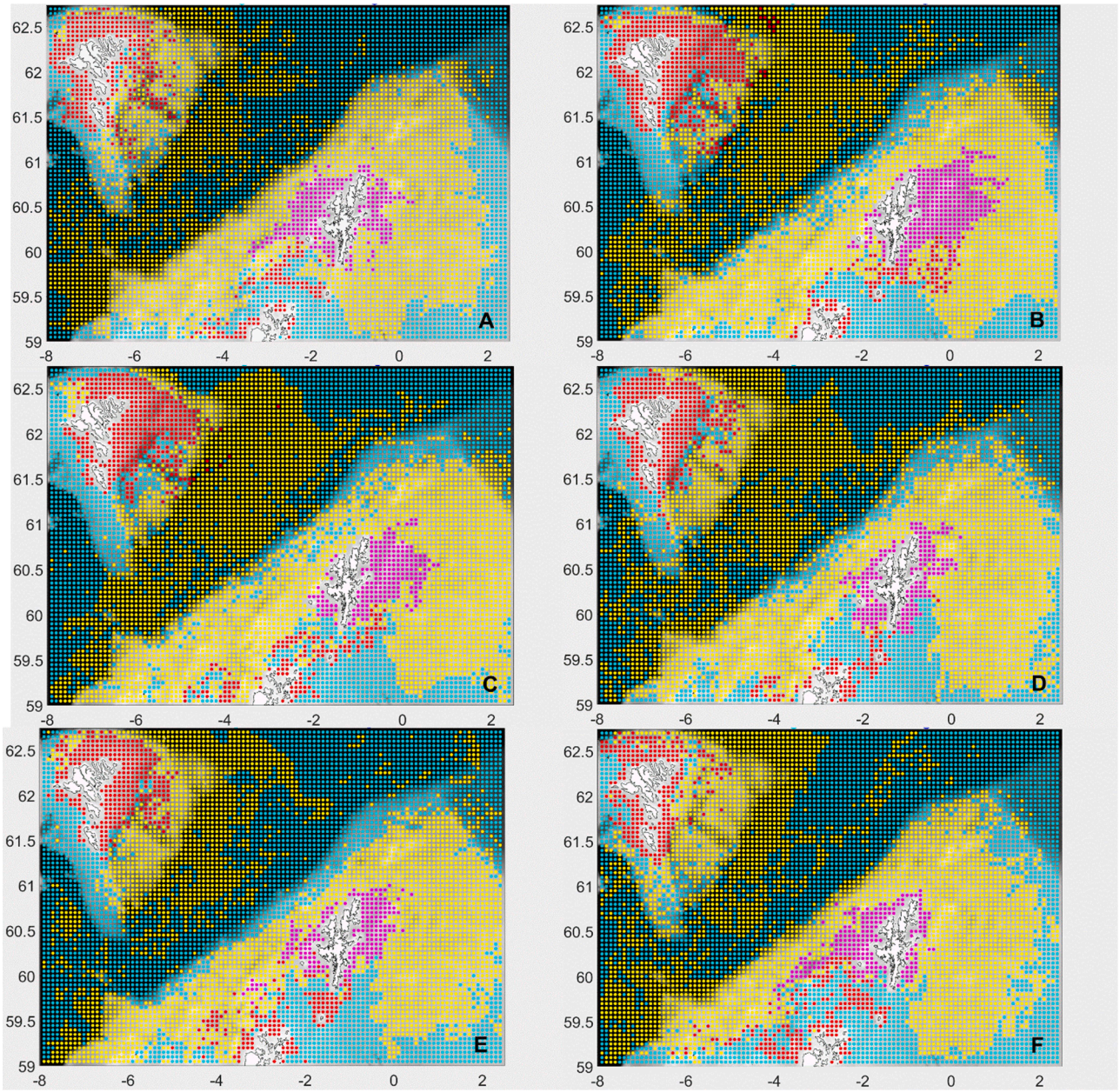

Fig. 5. As Fig. 4, except starting position of particles are from tracking models which have been run over 28 days starting from A 20th May 2007, B 3rd June 2007, C 17th June 2007, D 1st July 2007, E 15th July 2007, and F 29th July 2007.

all other years apart from 2018 ($p < 0.001$), but this was the only significant difference detected between years (Fig. 9).

3.3. Wind

There is a difference between summer winds during 2006 and 2018 and summer winds of all years (Fig. 10). The mean direction of winds during 2013 and 2018 was south-westerly more often than other directions, similar to other years (Fig. 10). In contrast to other years, though, the percentage of time that winds came from the Southwest was higher during 2013 and 2018, and mean wind speeds were higher during 2018 (Fig. 10). The strongest winds during the summer were detected in 2018 (Fig. 10).

3.4. Chlorophyll concentration around the Shetland Islands

Surface chlorophyll concentration has been displayed in an animated gif running from April until the end of September of each year from 2006 to 2018 (Dees, 2021b). Chlorophyll maps from other years also showed elevated concentrations around Shetland but most closely matched origin locations of particles in simulations (see Figs. 4–7) during 2018 (Fig. 11). Uncertainty values exceeding 50 %, and surface chlorophyll concentrations below 3 mg m^{-3}, were excluded from maps to maximise the potential utility of chlorophyll concentration estimates by showing maps from a maximum of two days before or after the start date of model simulations (Fig. 11). Enhanced chlorophyll concentrations were present along the west coast and southeast of mainland Scotland on 21st May 2018 (Fig. 11A). Particle tracking models indicated that theoretical particles which landed on Shetland in the four weeks after 21st May 2018) originated from east of Shetland (Fig. 7A).

A chlorophyll signal of approximately 10 mg m^{-3} was detected along the 200 m isobath west of Shetland on 4th June 2018 (Fig. 11B). Particle tracking models predicted that chlorophyll from this region would be advected towards the coast of Shetland, as several particles which

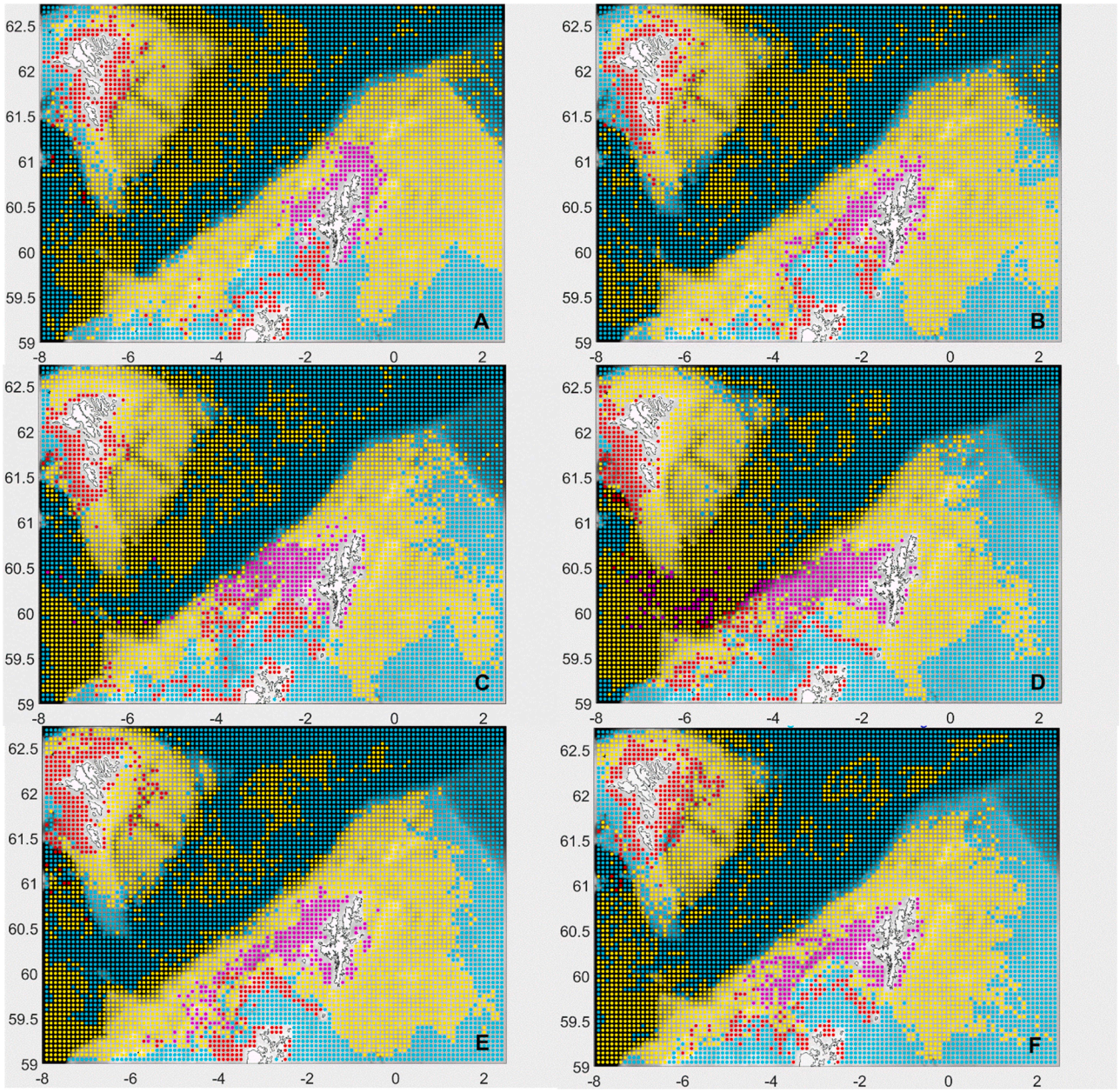

Fig. 6. As Fig. 4, except starting position of particles are from tracking models which have been run over 28 days starting from A 19th May 2013, B 2nd June 2013, C 16th June 2013, D 30th July 2013, E 14th July 2013, and F 28th July 2013.

landed on Shetland in particle tracking simulations originated from the same area that chlorophyll was detected by satellite sensors (Figs. 7B and 11B).

On 16th June 2018, no evidence of intense proliferation of chlorophyll was observed near Shetland (Fig. 11C). At the end of June 2018, however, high surface chlorophyll concentration was detected west of Shetland (Fig. 11D), closer to the Shetland west coast than at the beginning of June (Figs. 7B and D). At this time, chlorophyll appeared to be concentrated between the 200 m and 100 m isobaths west of Shetland, and most chlorophyll was not detected closer to the west coast of Shetland than the 100 m isobath (Fig. 11D).

4. Discussion

The first attempt to use a hydrodynamic model to evaluate the advection of harmful *Dinophysis* spp. blooms around the Scottish Shetland islands, an important site of shellfish aquaculture, has been presented here. The accuracy of the model close to the Shetland coastline is discussed using comparisons to data recorded by drifters. Findings of the model are then evaluated in the context of improving the prediction of HABs near Shetland to the benefit of aquaculture stakeholders in the region.

4.1. Model validation

The skill of the state of the art hydrodynamic model AMM15, and its previous iteration AMM7, have previously been verified for use over its entire domain (Graham et al., 2018; O'Dea et al., 2017). Results of particle tracking experiments have likewise recreated major oceanographic processes and surface water circulation (Table 1). Credibility of the model's representation of particle landings was demonstrated here by comparing drifters and particles during two periods (Fig. 3).

Modelled particles moved over a much wider area than drifters, particularly between May and June 2018 (Fig. 3). The differences in

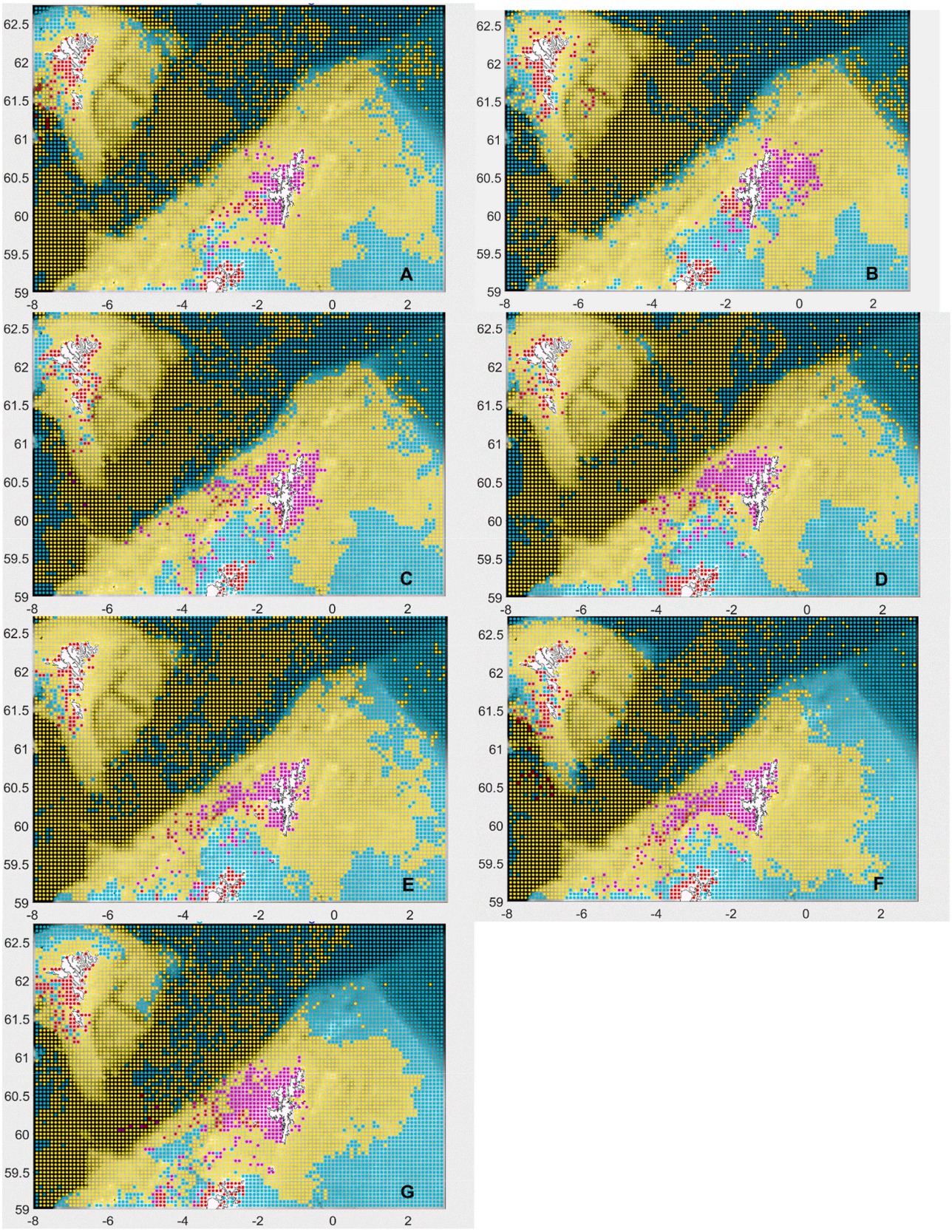

Fig. 7. As Fig. 4, except starting position of particles are from tracking models which have been run over 28 days starting from A 6th May 2018, B 20th May 2018, C 3rd June 2018, D 17th June 2018, E 1st July 2018, F 15th July 2018, and G 29th July 2018.

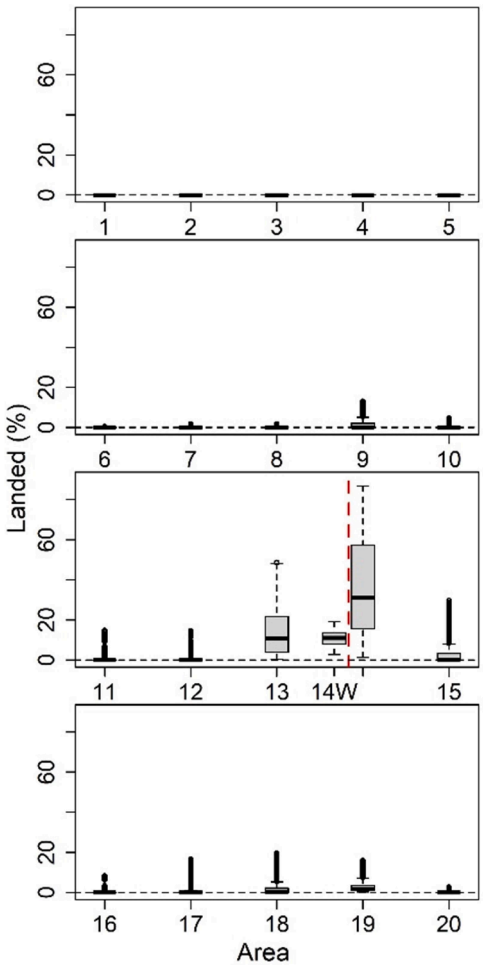

Fig. 8. The total percentage of particles landing on Shetland which originated from each region in the study area during all model simulations. Area names correspond to those specified in Fig. 1. The y-axis corresponds to the percentages of particles from each area which landed on Shetland during each of the 2880 model simulations completed during the study period. Boxplots were drawn from the combined 2880 model simulations; from 12 weeks over 10 years, repeated 24 times each. A red vertical line has been drawn to show the approximate location of Shetland.

tracks of modelled particles and drifters is to be expected; minor differences in starting position of modelled particles translated to large differences in final location (Lorenz, 1963; Thiétart and Forgues, 1995). The relatively similar tracks of particles and drifters in July also suggests any differences are due to chaotic dispersion under the influence of the random effect introduced in Eq. (1). A longer deployment time corresponded to a larger spread of modelled particles, and when the deployment period was shorter there is greater agreement between drifters and modelled particles (Fig. 3). This consistency between AMM15 modelled particles and drifter tracks in 2018 shows movement of modelled particles close to shore in simulations is credible, with movements both away from the coast and towards the coast being recreated by the model (Fig. 3; Dees, 2021). Results presented here are consistent with a previous comparison of drifters and AMM15 modelled particles in Scottish waters by Jones et al. (2020).

Although only two years, 2017 and 2018, of modelled velocities used here have undergone validation by the model's creators (Graham et al., 2018), *Dinophysis* spp. cell abundance records also suggests that modelled data from previous years is robust. The exceptional 2013 *Dinophysis* spp. bloom advected to Shetland by strong westerly winds (Whyte et al., 2014) appears to be reflected in results. Model output using 2013 velocities from AMM15 showed a greater number of particles landing on Shetland that had originated from west of Shetland (Fig. 6), likely due to increased south-westerly winds during the summer (Fig. 10). The successful simulation of this event demonstrates that trends have been recreated accurately and the model output is sensible.

4.2. Can hindcasts of past events inform our knowledge of HABs?

Elevated abundances of *Dinophysis* spp. were detected in the Shetland Islands during years 2006, 2007, 2013 and 2018 (Parks et al., 2019; Whyte et al., 2014; Fig. 2). The mean percentage of modelled particles which landed on Shetland from west of the islands was also higher during three of these four years: 2006, 2013 and 2018 (Fig. 9). Most shellfish farms in Shetland are located on its west coast and are therefore adversely affected by HABs advected from the west. Years during which high abundances of HABs were detected (Gillibrand et al., 2016; Whyte et al., 2014) were therefore more likely to coincide with years showing most particles landing on Shetland originated from west of Shetland (Figs. 4–7, Table 1).

Previous studies have shown *Dinophysis* spp. abundance in Shetland was significantly higher than the mean abundance during the period 2006 – 2013 in both 2006 and 2013 (Whyte et al., 2014). The mean *Dinophysis* spp. abundance remained significantly higher for a longer period during 2006, but the actual abundance was highest during 2013 (Whyte et al., 2014). Particle tracking simulations corroborate this finding (Fig. 9A), as the mean percentage of particles landing on Shetland which originated from Area 13 were also higher than average for more weeks during 2006 than 2013 (Fig. 9A). Whyte et al. (2014) postulated that westerly currents driven by elevated westerly winds during the summers of 2006 and 2013 were responsible for rapidly advected toxic *Dinophysis* spp. blooms. Our results also show eastward surface currents were likely to have been influenced by the greater proportion of south-westerly winds during 2013 (Fig. 10). The percentage of particles originating from Area 13 during 2006 was exceptionally high for a greater number of weeks than during any other year, but higher percentages of particles landing on Shetland were modelled during weeks 26 – 28 of 2013 (Fig. 9). This again mirrors *Dinophysis* spp. abundance trends during 2006 – 2013 (Whyte et al., 2014).

A high percentage of modelled particles landing on Shetland does not always indicate that a large abundance of *Dinophysis* spp. was detected, and higher *Dinophysis* spp. abundances are not always preceded by higher numbers of modelled particles landing on Shetland. *Dinophysis* spp. abundance also exceeded 5000 cells L^{-1} during 2007 and 2018 (Fig. 2; Parks et al., 2019), and statistical testing showed *Dinophysis* spp. abundance was significantly higher during 2018 than all years apart from 2006 during May and June (Dees, 2021c; Parks et al., 2019). *Dinophysis* spp. abundance during 2007 was not significantly higher despite exceeding the 5000 cells L^{-1} threshold used for this study (Fig. 2). Conversely, the origins of modelled particles which landed in Shetland during May 2018 were relatively close to Shetland, compared to particles modelled after June (Fig. 7), and the mean percentage of landed particles which originated from Area 13 was only significantly higher during the first two weeks of June (Fig. 9). Consistently high percentages of particles landing on Shetland from Area 13 were not found during 2007 (Fig. 5). Several reasons for the difference between the numbers of modelled particles landing on Shetland and the abundance of *Dinophysis* spp. detected at the coast during 2007 and 2018 can be suggested here.

Firstly, the particle tracking model used in the present study does not attempt to include biologically realistic processes such as reproduction or cell death. Model simulations were limited to lasting a total of four weeks for this reason, but this by necessity means the beginning and end of simulated blooms are highly rigid, which is not likely to be observed in the natural world. Including biologically relevant processes in the future may improve the accuracy of similar models.

Other biological processes detected in dinoflagellates may also need to be included in future models. For example, a number of dinoflagellate

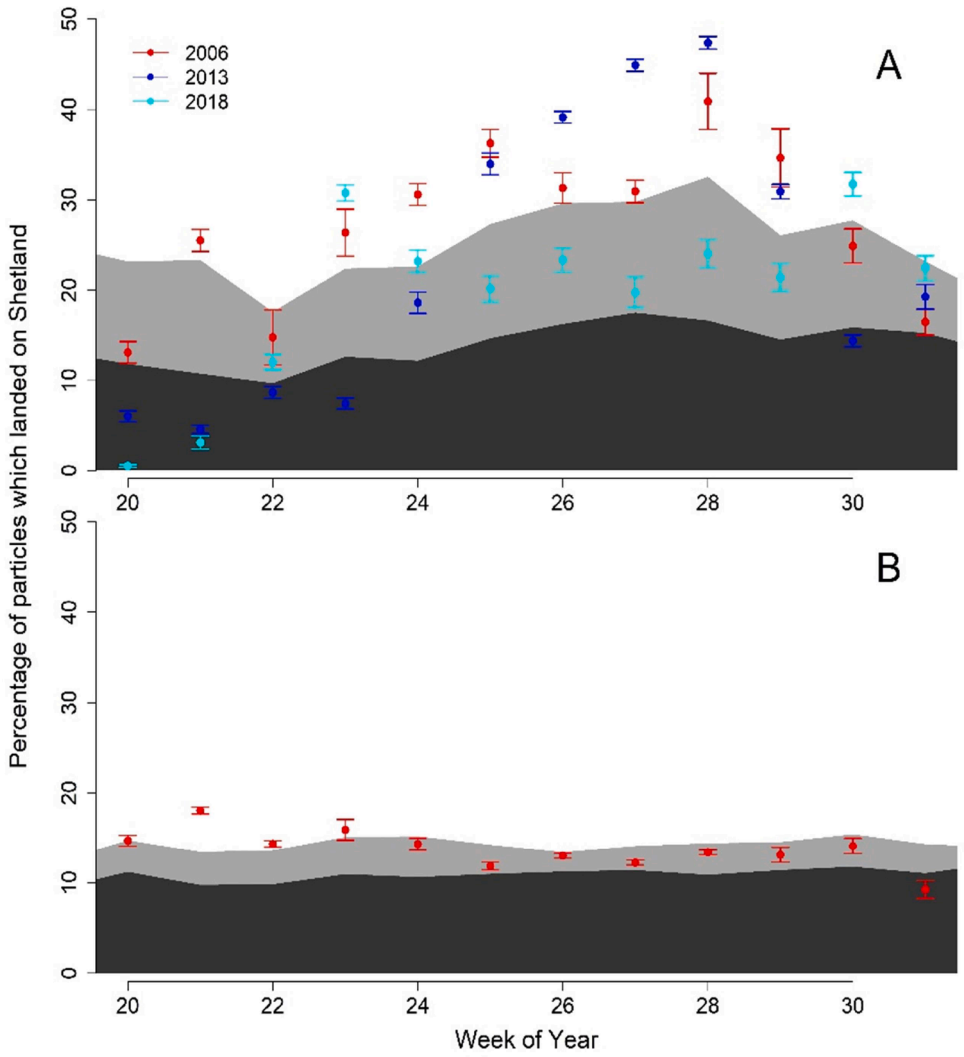

Fig. 9. Mean percentages of particles landing on Shetland which originated from A Area 13 and B Area 14W, during years 2006 – 2013 and 2016 - 2018 for specific weeks of the year. Week number 19 corresponds to the first week of May and week 33 corresponds to the third week of August, using Sunday as the first day of the week. The mean percentage of particles which landed on Shetland for each week number for all years in the study are displayed in dark grey; the additional standard deviations are displayed in light grey. Individual coloured points show the mean (+/- standard deviation) of percentages of particles landing on Shetland during A 2006, 2013 and 2018, and B 2006. Only 2006 is displayed separately in B because it was the only year significantly different from all other years apart from 2018 (pairwise t-tests, $p < 0.001$).

genera implicated in toxin producing or high biomass HABs have been shown to form cyst beds along the western coast of mainland Scotland and Shetland, including *Alexandrium* spp. and *Lingulodinium* spp. (Brown et al., 2010; Lewis, 1988; Lewis et al., 1995). Cysts beds of *Alexandrium* spp. contribute to annual toxic blooms in Alaska (Anderson et al., 2021) and elsewhere, but a similar process is unlikely to be responsible for enhanced *Dinophysis* spp. blooms as cyst production by *Dinophysis* spp. has not been reliably demonstrated (Reguera et al., 2012). Other conditions are more likely to have affected the abundance of *Dinophysis* spp. near Shetland during 2007 and 2018, such as temperature (Gobler et al., 2017), species diversity (Paterson et al., 2017; Swan et al., 2018), or the availability of prey (Park et al., 2006). Further examination of past physical data may reveal reasons for the enhanced abundance during 2007 and the beginning of 2018.

Commenting further on the ecology of HABs around Shetland, and whether HABs arrive on Shetland purely due to advection by currents or whether they also need to have a sufficiently large cell abundance to be transported, is beyond the scope of this study. As the dataset collected by the coastal monitoring system becomes larger, enough data may be gathered to compare bloom and non-bloom years sufficiently. In this paper, finding whether particular areas around Shetland are prone to accumulations of HAB species and finding ways to predict the arrival of these blooms at the coast will be focussed on.

Chlorophyll maps show that increased chlorophyll concentrations are detectable at the ocean surface in the locations where particle tracking models indicate algal blooms originated (Dees, 2021b). The likelihood of using erroneous chlorophyll data was reduced in the current study, by removing data associated with an error value of greater than 50 %. Chlorophyll maps show, however, that during 2018 chlorophyll was concentrated along the 100 m and 200 m isobaths west of Shetland (Fig. 11C + 11D). The particle tracking model shows it is likely some of this chlorophyll was advected to the Shetland coast (Fig. 7*D* and E). The 200 m isobath shows the approximate edge of the continental slope where the ESC is often found. Previous studies examining the movement and development of dinoflagellate dominated HABs like the 2006 *K. mikimotoi* bloom, used chlorophyll maps and particle tracking models to show that ESC can be an important pathway for dinoflagellate transport (Gillibrand et al., 2016; Siemering et al., 2016). Evidence of fronts forming at the 100 m isobath west of Shetland has also been found (Dees, 2021c; Hughes, 2014), further showing that frontal regions are

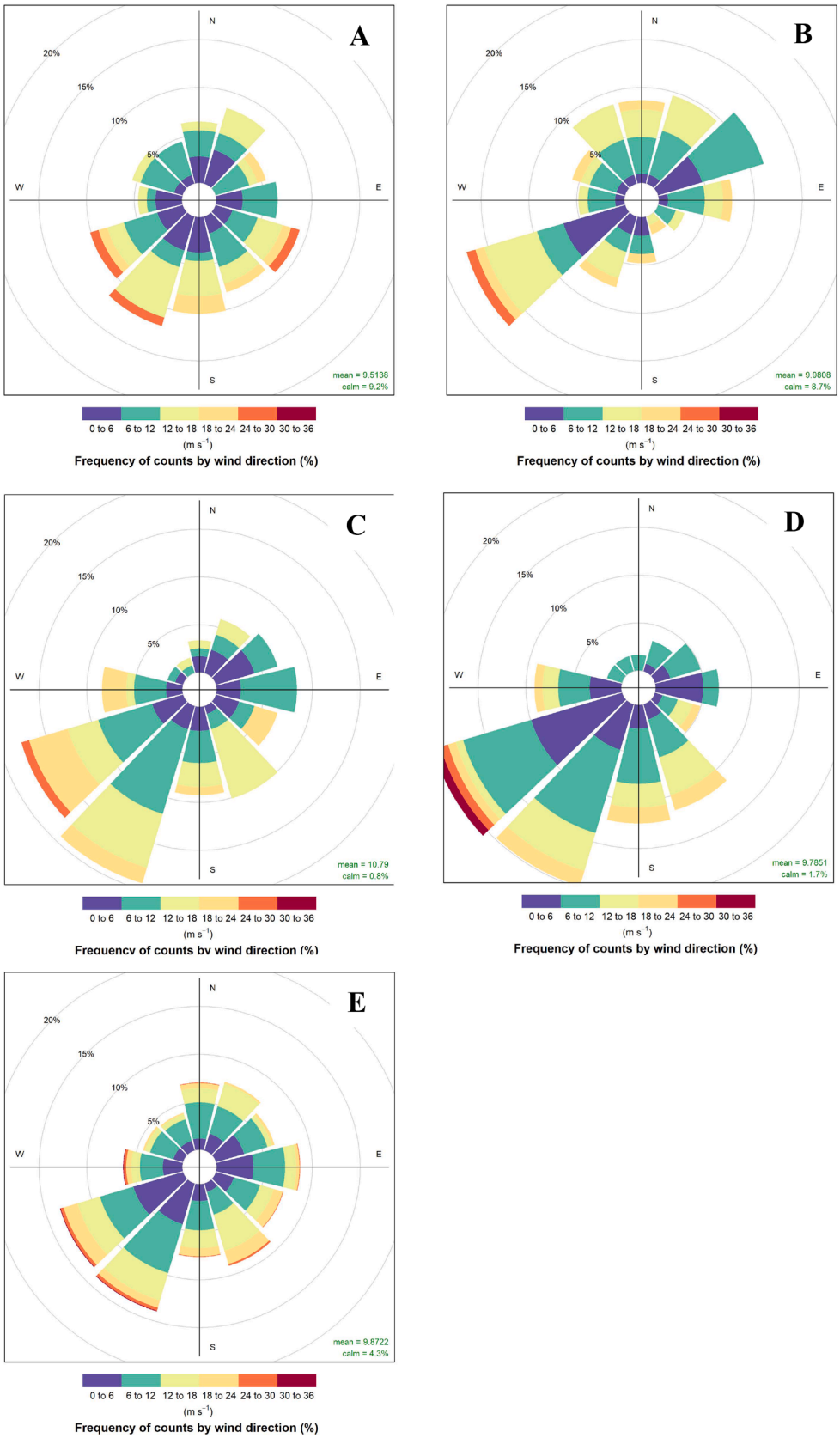

Fig. 10. Wind roses showing hourly-averaged wind speed and direction for summers of A 2006, B 2007, C 2013, D 2018, and E all years in the study period.

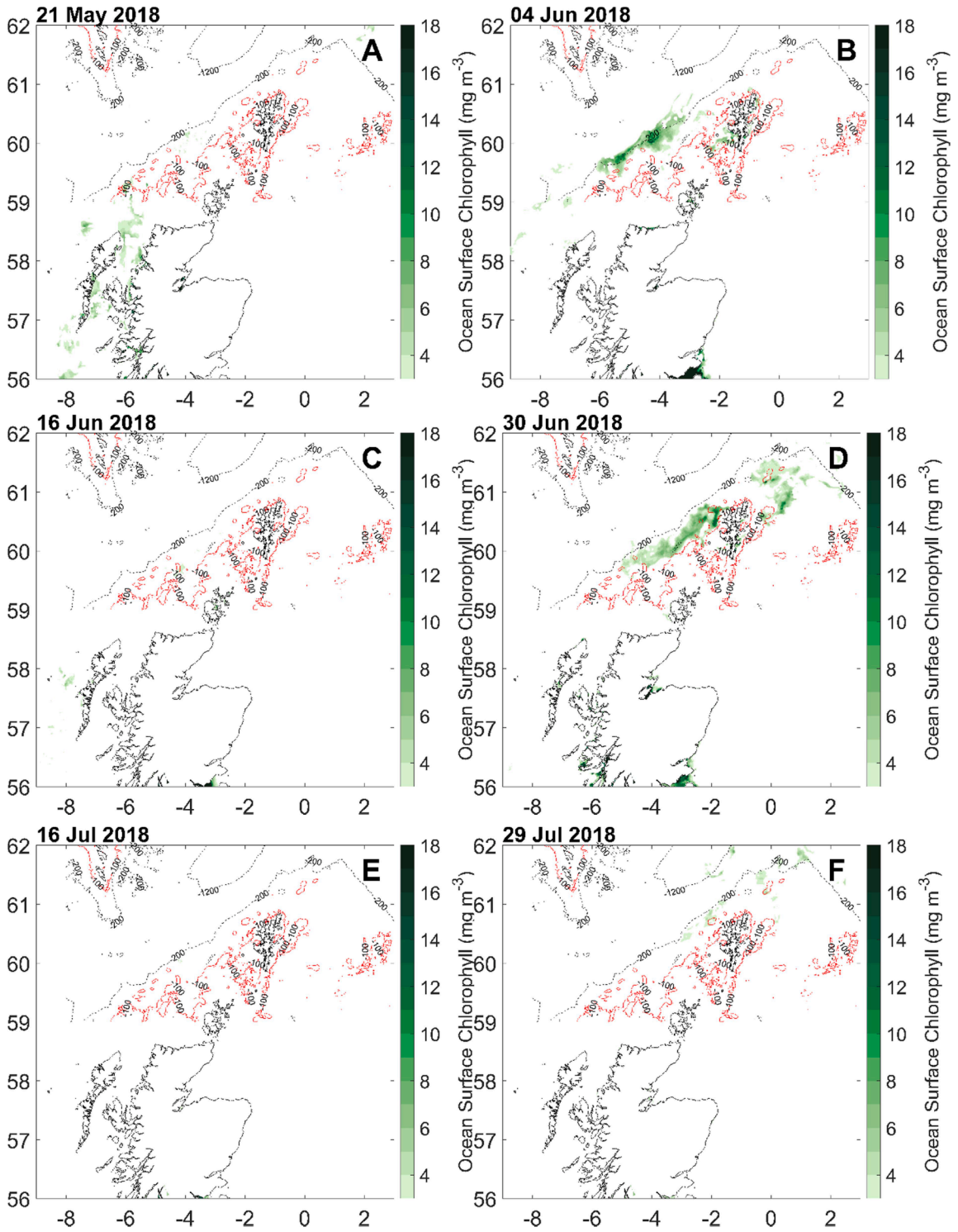

Fig. 11. Modelled 1 km^2 resolution of surface chlorophyll as estimated by the merged product by the ACRI-ST Company during 2018. This chlorophyll product has not undergone interpolation in cloud obscured areas, and values associated with an error value of over 50 % have not been plotted (see methods). Modelled area is bounded by 55° and 62.74° N, and −12° and 2.5° E. Different starting dates, which are labelled by A, B, C, D, E and F, correspond to the starting dates of particle tracking models in Fig. 7. The 100 m isobath has been drawn in red line, and the 200 m and 1200 m isobaths are plotted using dotted black lines.

important for the formation and advection of HABs (Franks, 1992a; Paterson et al., 2017; Siemering et al., 2016).

Dinophysis spp. HABs can exist at relatively low cell densities (Fig. 2); they are therefore unlikely to be directly observed using remote sensing technology (Davidson et al., 2016; Parks et al., 2019). The fact that high abundances of algae are not always necessary for the production of toxins means that using satellite chlorophyll data in conjunction with particle tracking forecasts will result in false negatives (Stumpf et al., 2009, 2003). The differences in results from 2006 to 2013, and 2007 and 2018, also show relying on only these data sources can be inadequate for an effective EWS. Using these data sources in combination with routine coastal phytoplankton and toxin monitoring, however, should reduce the rate of both false positives and false negatives (Davidson et al., 2021).

Although it is likely impossible to directly detect HABs composed of *Dinophysis* spp. using satellite estimates of photosynthetic pigments, detecting *Dinophysis* spp. by proxy may be possible. The photosynthetic ciliate *Mesodinium rubrum* has been identified as a prey species of *D. acuminata* (Park et al., 2006; Riisgaard and Hansen, 2009), the dominant *Dinophysis* species in Scottish waters (Hart et al., 2007; Paterson et al., 2017; Swan et al., 2018). Large blooms of *M. rubrum* can be detected remotely, as large cell abundances can cause red tides (Garcia et al., 1993; Guzmán et al., 2016). Although *M. rubrum* has a widespread distribution, assessing its abundance in the water column is not simple and other species around Scotland and the Shetland Islands may be more likely to form red tides than this ciliate (Crawford, 1989; Wyatt and Zingone, 2014). Future studies of the co-occurrence of *M. rubrum* and *Dinophysis* spp. around Shetland may determine whether using such a proxy is a good idea.

One novel finding of this study is the results of model simulations being plotted on a map to show the range of percentages which landed on the Shetland coast from each area (Fig. 8). Observing changes in the percentages of theoretical particles landing on Shetland can give greater meaningful information than results from a single simulation. Particle tracking models have shown that there are very few instances when the percentage of particles originating from Areas 14W or 14E which landed on Shetland was zero (Fig. 8). It is therefore highly likely that HABs detected in these areas will land on Shetland within less than a month. This is in agreement with previous studies hypothesising that most HABs landing on Shetland are advected from west of the archipelago (Gillibrand et al., 2016; Whyte et al., 2014). The percentage of particles from these areas which landed on Shetland did not reach 100 % (Fig. 8), suggesting the exact location of HABs in each area is important. Repeating model simulations of particles in Areas 14E and 14 W only, will help clarify locations most important for HAB initiation. Repeated model simulations of smaller areas will determine the importance of the two frontal regions along the 100 m and 200 m isobaths for HAB advection, and will confirm the best location to place smart offshore HAB early warning sensors.

Further studies should also determine how sensitive particle diffusion is, by measuring how the percentage of particles which originate from these areas landing on Shetland varies with changes in the random diffusive effect from Eq. (1). This will be a useful avenue of research, and will improve robustness of the model, particularly as higher resolution models become available. There is little variation in the percentage of particles from Area 14 W which landed on Shetland, suggesting that when a HAB is suspected between the coast and −2° East there is a high likelihood of it being advected towards Shetland, regardless of the direction of winds or currents (Figs. 8, 9).

Observing chlorophyll maps alongside abundances of potentially toxin producing species of phytoplankton can thus be highly useful. This study shows the benefit of providing warnings when chlorophyll maps indicate there are blooms near Shetland (Davidson et al., 2021). It will be helpful in the future to assess the phytoplankton groups which are most likely to coincide with *Dinophysis* spp., to develop a system whereby chlorophyll maps may be characterised as harmful or not. Interest is growing in finfish aquaculture stakeholders in addition to those primarily involved in shellfish aquaculture. The size of the finfish aquaculture industry is much larger than that for shellfish (Davidson et al., 2021). Because of this, the focus of HAB modelling focusses not only on toxin producing dinoflagellates such as *Dinophysis* spp. and *Alexandrium* spp., but also spiny chain forming diatoms like *Chaetoceros* spp. and the *delicatissima* subgroup of *Pseudo-nitzschia* (Davidson et al., 2021). Using chlorophyll maps to track high biomass blooms is generally easier due to the larger cell densities involved (Shutler et al., 2012; Sourisseau et al., 2016). Developing algorithms to distinguish toxin producing blooms from high-biomass blooms is therefore being focussed on by some groups, which will provide further interest to future modelling studies (Kurekin et al., 2014; Martinez-Vicente et al., 2020; Mateus et al., 2019).

5. Conclusions

This study shows the use of a particle tracking model to hindcast pathways of advected HABs impacting coastal aquaculture in the Scottish Shetland Islands. The present study has shown that water currents are important for the advection of HABs, and using satellite imagery with particle tracking models can usefully supplement coastal microscope-based counts of HAB cell abundance to enhance prediction of HAB events. Further repeated model simulations will guide researchers to the best place around Shetland to place targeted HAB sensors, as part of a 21st Century EWS.

During three of the four *Dinophysis* bloom years of 2006, 2013 and 2018, most particles landing on the Shetland coastline originated from west of the archipelago (Figs. 4, 6 and 7). It was previously thought that westerly winds during the *Dinophysis* spp. growth season were a harbinger for coming HABs (Whyte et al., 2014). The present analysis has confirmed this hypothesis, as well as showing that these HABs can originate relatively far from the Shetland coastline, potentially providing time for mitigation measures to be put in place before they impact.

Declaration of Competing Interest

The authors declare that they have no known competing financial interests or personal relationships that could have appeared to influence the work reported in this paper.

Acknowledgements

Funding for this work came from a PhD studentship from the European Social Fund and University of the Highlands and Islands (UHI_SAMS_DSW_PGR_AY16/17). KD and AD were funded by the UKRI project: Evaluating the Environmental Conditions required for the Development of Offshore Aquaculture (Off-Aqua) BB/S004246/1. PD also acknowledges funding from the European Union's Horizon 2020 research and innovation programme under the Marie Skłodowska-Curie grant agreement No 101034309. MASTS small grant No. SG401 was used to purchase three SouthTEK Sensing Technologies Offshore Nomad drifters used in this study. We are also grateful to the crew of the RV *Moder Dy* who provided practical assistance in fieldwork, and the population of the Shetland Islands who helped look out for drifters. Cathy King has been especially helpful when discussing cysts around Shetland. We would like to thank the two anonymous reviewers who gave helpful feedback and suggestive edits to improve this manuscript.

References

Aleynik, D., Dale, A.C., Porter, M., Davidson, K., 2016. A high resolution hydrodynamic model system suitable for novel harmful algal bloom modelling in areas of complex coastline and topography. Harmful Algae 53, 102–117. https://doi.org/10.1016/j.hal.2015.11.012.

Anderson, D.M., Fachon, E., Pickart, R.S., Lin, P., Fischer, A.D., Richlen, M.L., Uva, V., Brosnahan, M.L., McRaven, L., Bahr, F., Lefebvre, K., Grebmeier, J.M., Danielson, S. L., Lyu, Y., Fukai, Y., 2021. Evidence for massive and recurrent toxic blooms of *Alexandrium catenella* in the Alaskan Arctic. Proc. Natl. Acad. Sci. U. S. A. 118 https://doi.org/10.1073/pnas.2107387118.

Berdalet, E., Fleming, L.E., Gowen, R., Davidson, K., Hess, P., Backer, L.C., Moore, S.K., Hoagland, P., Enevoldsen, H., 2016. Marine harmful algal blooms, human health and wellbeing: challenges and opportunities in the 21st century. J. Mar. Biol. Assoc. United Kingdom 96, 61–91. https://doi.org/10.1017/S0025315415001733.

Bolado-Penagos, M., Gomiz-Pascual, J., Vázquez, A., Bruno, M., Arruda, R., Calil, P., Caldeira, R.M.A., 2017. Microstructure turbulence profiles at the Gibraltar Strait. Liege Colloquium on Ocean Dynamics 2017. https://doi.org/10.13140/RG.2.2.11263.00166.

Bresnan, E., Arévalo, F., Belin, C., Branco, M.A.C., Cembella, A.D., Clarke, D., Correa, J., Davidson, K., Dhanji-Rapkova, M., Lozano, R.F., Fernández-Tejedor, M., Guðfinnsson, H., Carbonell, D.J., Laza-Martinez, A., Lemoine, M., Lewis, A.M., Menéndez, L.M., Maskrey, B.H., McKinney, A., Pazos, Y., Revilla, M., Siano, R., Silva, A., Swan, S., Turner, A.D., Schweibold, L., Provoost, P., Enevoldsen, H., 2021. Diversity and regional distribution of harmful algal events along the Atlantic margin of Europe. Harmful Algae 102. https://doi.org/10.1016/j.hal.2021.101976.

Brown, L., Bresnan, E., Graham, J., Lacaze, J.-P.P., Turrell, E., Collins, C., 2010. Distribution, diversity and toxin composition of the genus *Alexandrium* (Dinophyceae) in Scottish waters. Eur. J. Phycol. 45, 375–393. https://doi.org/10.1080/09670262.2010.495164.

Chen, C., Beardsley, R.C., Cowles, G., Qi, J., Lai, Z., Gao, G., Stuebe, D., Xu, Q., Xue, P., Ge, J., Ji, R., Hu, S., Tian, R., Huang, H., Wu, L., Lin, H., 2011. An unstructured-grid, finite-volume community ocean model FVCOM user manual. FVCOM User Man.

Crawford, D., 1989. *Mesodinium rubrum*: the phytoplankter that wasn't. Mar. Ecol. Prog. Ser. 58, 161–174. https://doi.org/10.3354/meps058161.

Davidson, K., Anderson, D.M., Mateus, M., Reguera, B., Silke, J., Sourisseau, M., Maguire, J., 2016. Forecasting the risk of harmful algal blooms. Harmful Algae 53, 1–7. https://doi.org/10.1016/j.hal.2015.11.005.

Davidson, K., Whyte, C., Aleynik, D., Dale, A., Gontarek, S., Kurekin, A.A., Mcneill, S., Miller, P.I., Porter, M., Saxon, R., Swan, S., Iriarte, J.L., Stern, R.F., 2021. HABreports: online early warning of harmful algal and biotoxin risk for the Scottish shellfish and finfish aquaculture industries. Front. Mar. Sci. 8, 1–19. https://doi.org/10.3389/fmars.2021.631732.

Dees, P., (2021a). Particle tracking model simulations with drifters. https://doi.org/https://doi.org/10.6084/m9.figshare.16989304.

Dees, P., (2021b). Chlorophyll around Shetland from 2006 - 2018. https://doi.org/10.6084/m9.figshare.16989055.v1.

Dees, P., 2021c. Improving the Predictability of Harmful Algal Blooms Around the Shetland Islands. University of the Highlands and Islands.

Franks, P.J.S., 1992a. Sink or swim: accumulation of biomass at fronts. Mar. Ecol. Prog. Ser. 82, 1–12. https://doi.org/10.3354/meps082001.

Franks, P.J.S., 1992b. Phytoplankton blooms at fronts: patterns, scales, and physical forcing mechanisms. Rev. Aquat. Sci.

Franks, P.J.S., Walstad, L.J., 1997. Phytoplankton patches at fronts: a model of formation and response to wind events. J. Mar. Res. 55, 1–29. https://doi.org/10.1357/0022240973224472.

Garcia, C.A.E., Purdie, D.A., Robinson, I.S., 1993. Mapping a bloom of the photosynthetic ciliate *Mesodinium rubrum* in an estuary from airbourne thematic mapper data. Estuar. Coast. Shelf Sci. 37, 287–298.

Garnesson, P., Mangin, A., Bretagnon, M., 2021. Ocean colour production centre satellite observation global products. Qual. Inf. Doc. 1–93.

Gianella, F., Burrows, M.T., Swan, S.C., Turner, A.D., Davidson, K., 2021. Temporal and spatial patterns of harmful algae affecting Scottish shellfish aquaculture. Front. Mar. Sci. 8 https://doi.org/10.3389/fmars.2021.785174.

Giddings, S.N., MacCready, P., Hickey, B.M., Banas, N.S., Davis, K.A., Siedlecki, S.A., Trainer, V.L., Kudela, R.M., Pelland, N.A., Connolly, T.P., 2014. Hindcasts of potential harmful algal bloom transport pathways on the Pacific Northwest coast. J. Geophys. Res. Ocean. 119, 2439–2461. https://doi.org/10.1002/2013JC009622. Received.

Gillibrand, P.A., Siemering, B., Miller, P.I., Davidson, K., 2016. Individual-based modelling of the development and transport of a *Karenia mikimotoi* bloom on the North-west European continental shelf. Harmful Algae 53, 118–134. https://doi.org/10.1016/j.hal.2015.11.011.

Gobler, C.J., Doherty, O.M., Hattenrath-Lehmann, T.K., Griffith, A.W., Kang, Y., Litaker, R.W., 2017. Ocean warming since 1982 has expanded the niche of toxic algal blooms in the North Atlantic and North Pacific oceans. Proc. Natl. Acad. Sci. 114, 4975–4980. https://doi.org/10.1073/pnas.1619575114.

Graham, J.A., O'Dea, E., Holt, J., Polton, J., Hewitt, H.T., Furner, R., Guihou, K., Brereton, A., Arnold, A., Wakelin, S., Sanchez, J.M.C., Adame, C.G.M., 2018. AMM15: a new high-resolution NEMO configuration for operational simulation of the European north-west shelf. Geosci. Model Dev. 11, 681–696. https://doi.org/10.5194/gmd-11-681-2018.

Guzmán, L., Varela, R., Muller-Karger, F., Lorenzoni, L., 2016. Bio-optical characteristics of a red tide induced by *Mesodinium rubrum* in the Cariaco Basin, Venezuela. J. Mar. Syst. 160, 17–25. https://doi.org/10.1016/j.jmarsys.2016.03.015.

Hart, M.C., Green, D.H., Bresnan, E., Bolch, C.J., (2007). Large subunit ribosomal RNA gene variation and sequence heterogeneity of *Dinophysis* (Dinophyceae) species from Scottish coastal waters 6, 271–287. https://doi.org/10.1016/j.hal.2006.10.001.

Hill, A.E., Horsburgh, K.J., Garvine, R.W., Gillibrand, P.A., Slesser, G., Turrell, W.R., Adams, R.D., 1997. Observations of a density-driven recirculation of the Scottish coastal current in the Minch. Estuar. Coast. Shelf Sci. 45, 473–484. https://doi.org/10.1006/ecss.1996.0198.

Hinder, S.L., Hays, G.C., Edwards, M., Roberts, E.C., Walne, A.W., Gravenor, M.B., 2012. Changes in marine dinoflagellate and diatom abundance under climate change. Nat. Clim. Chang. 2, 271–275. https://doi.org/10.1038/nclimate1388.

Hopper, T., (2014). Windrose: supports the creation and plotting of rose plots for wind data.

Hu, C., Lee, Z., Franz, B., 2012. Chlorophyll a algorithms for oligotrophic oceans: a novel approach based on three-band reflectance difference. J. Geophys. Res. Ocean. 117, 1–25. https://doi.org/10.1029/2011JC007395.

Hughes, S., (2014). Inflow of Atlantic water to the north sea : seasonal variability on the east Shetland Shelf. University of the Highlands and Islands (UHI), under the terms of accreditation agreed with the University of Aberdeen.

Jones, S., Inall, M., Porter, M., Graham, J.A., Cottier, F., 2020. Storm-driven across-shelf oceanic flows into coastal waters. Ocean Sci. 16, 389–403. https://doi.org/10.5194/os-16-389-2020.

Kurekin, A.A., Miller, P.I., Van der Woerd, H.J., 2014. Satellite discrimination of *Karenia* mikimotoi and *Phaeocystis* harmful algal blooms in European coastal waters: merged classification of ocean colour data. Harmful Algae 31, 163–176. https://doi.org/10.1016/j.hal.2013.11.003.

Le Traon, P.Y., Antoine, D., Bentamy, A., Bonekamp, H., Breivik, L.A., Chapron, B., Corlett, G., Dibarboure, G., Digiacomo, P., Donlon, C., Faugère, Y., Font, J., Girard-Ardhuin, F., Gohin, F., Johannessen, J.A., Kamachi, M., Lagerloef, G., Lambin, J., Larnicol, G., Borgne, P.Le, Leuliette, E., Lindstrom, E., Martin, M.J., Maturi, E., Miller, L., Mingsen, L., Morrow, R., Reul, N., Rio, M.H., Roquet, H., Santoleri, R., Wilkin, J., 2015. Use of satellite observations for operational oceanography: recent achievements and future prospects. J. Oper. Oceanogr. 8, s12–s27. https://doi.org/10.1080/1755876X.2015.1022050.

Levene, H., 1960. Robust tests for equality of variances. In: Olkin, I. (Ed.), Contributions to Probability and Statistics: Essays in Honor of Harold Hotelling. Stanford University Press, Stanford, pp. 278–292.

Lewis, J., 1988. Cysts and sediments: Gonyaulax polyedra (Lingulodinium Machaerophorum) in Loch Creran. J. Mar. Biol. Assoc. United Kingdom 68, 701–714. https://doi.org/10.1017/S0025315400028812.

Lewis, J., Higman, W., Kuenstner, S., 1995. Occurrence of *Alexandrium* sp. cysts in sediments from the North East coast of Britain. In: Lassus, P., Arzul, G., Erard, E., Gentien, P., Marcaillou, C. (Eds.), Harmful Marine Algal Blooms. Lilly. Lavoisier, Paris, pp. 175–180.

Li, Y., He, R., McGillicuddy, D.J., Anderson, D.M., Keafer, B.A., 2009. Investigation of the 2006 *Alexandrium fundyense* bloom in the Gulf of Maine: in-situ observations and numerical modeling. Cont. Shelf Res. 29, 2069–2082. https://doi.org/10.1016/j.csr.2009.07.012.

Lorenz, E., 1963. Deterministic nonperiodic flow. J. Atmos. Sci. 20, 130–141. https://doi.org/10.1201/9780203734636-38.

Maguire, J., Cusack, C., Ruiz-Villarreal, M., Silke, J., McElligott, D., Davidson, K., 2016. Applied simulations and integrated modelling for the understanding of toxic and harmful algal blooms (ASIMUTH): integrated HAB forecast systems for Europe's Atlantic Arc. Harmful Algae 53, 160–166. https://doi.org/10.1016/j.hal.2015.11.006.

Martinez-Vicente, V., Kurekin, A., Sá, C., Brotas, V., Amorim, A., Veloso, V., Lin, J., Miller, P.I., 2020. Sensitivity of a satellite algorithm for harmful algal bloom discrimination to the use of laboratory bio-optical data for training. Front. Mar. Sci. 7, 1–13. https://doi.org/10.3389/fmars.2020.582960.

Martino, S., Gianella, F., Davidson, K., 2020. An approach for evaluating the economic impacts of harmful algal blooms: the effects of blooms of toxic *Dinophysis* spp. on the productivity of Scottish shellfish farms. Harmful Algae 99, 1–12. https://doi.org/10.1016/j.hal.2020.101912.

Mateus, M., Fernandes, J., Revilla, M., Ferrer, L., Villarreal, M.R., Miller, P.I., Schmidt, W., Maguire, J., Silva, A., Pinto, L., 2019. Early warning systems for shellfish safety: the pivotal role of computational science. In: Rodrigues, J. (Ed.), International Conference on Computational Science. Springer, pp. 361–375. https://doi.org/10.1007/978-3-030-22747-0_28.

Mateus, M., Riflet, G., Chambel, P., Fernandes, L., Fernandes, R., Juliano, M., Campuzano, F., De Pablo, H., Neves, R., 2012. An operational model for the West Iberian coast: products and services. Ocean Sci. 8, 713–732. https://doi.org/10.5194/os-8-713-2012.

O'Dea, E., Furner, R., Wakelin, S., Siddorn, J., While, J., Sykes, P., King, R., Holt, J., Hewitt, H., 2017. The CO5 configuration of the 7 km Atlantic margin model: large-scale biases and sensitivity to forcing, physics options and vertical resolution. Geosci. Model Dev. 10, 2947–2969. https://doi.org/10.5194/gmd-10-2947-2017.

O'Reilly, J.E., Maritorena, S., Mitchell, B.G., Siegel, D.A., Carder, K.L., Garver, S.A., Kahru, M., McClain, C., 1998. Ocean color chlorophyll algorithms for SeaWiFS. J. Geophys. Res. Ocean. 103, 24937–24953. https://doi.org/10.1029/98JC02160.

Park, M.G., Kim, S., Kim, H.S., Myung, G., Kang, Y.G., Yih, W., 2006. First successful culture of the marine dinoflagellate *Dinophysis acuminata*. Aquat. Microb. Ecol. 45, 101–106. https://doi.org/10.3354/ame045101.

Parks, R., Swan, S., Davidson, K., Turner, A., Maskrey, B., Powell, A., Ford, C., Petch, R. G., (2019). Annual report on the results of the Biotoxin and Phytoplankton Official Control Monitoring Programmes for Scotland - 2018.

Paterson, R.F., Mcneill, S., Mitchell, E., Adams, T.P., Swan, S.C., Clarke, D., Miller, P.I., Bresnan, E., Davidson, K., 2017. Environmental control of harmful dinoflagellates and diatoms in a fjordic system. Harmful Algae 69, 1–17. https://doi.org/10.1016/j.hal.2017.09.002.

Pinto, L., Mateus, M., Silva, A., 2016. Modeling the transport pathways of harmful algal blooms in the Iberian coast. Harmful Algae 53, 8–16. https://doi.org/10.1016/j.hal.2015.12.001.

Raine, R., Cosgrove, S., Fennell, S., Gregory, C., Barnett, M., Purdie, D., Cave, R., 2017. Origins of *Dinophysis* blooms which impact Irish aquaculture. In: Proceedings of the 17th International Conference on Harmful Algae. International Society for the Study of Harmful Algae, pp. 46–49, 2017. Florianópolis, Brazil.

Reguera, B., Velo-Suárez, L., Raine, R., Park, M.G., 2012. Harmful *Dinophysis* species: a review. Harmful Algae 14, 87–106. https://doi.org/10.1016/j.hal.2011.10.016.

Ribotti, A., Antognarelli, F., Cucco, A., Falcieri, M.F., Fazioli, L., Ferrarin, C., Olita, A., Oliva, G., Pes, A., Quattrocchi, G., Satta, A., Simeone, S., Tedesco, C., Umgiesser, G., Sorgente, R., 2018. An operational marine oil spill forecasting tool for the management of emergencies in the Italian seas. J. Mar. Sci. Eng. 7 https://doi.org/10.3390/jmse7010001.

Riisgaard, K., Hansen, P.J., 2009. Role of food uptake for photosynthesis, growth and survival of the mixotrophic dinoflagellate *Dinophysis acuminata*. Mar. Ecol. Prog. Ser. 381, 51–62. https://doi.org/10.3354/meps07953.

Shutler, J.D., Davidson, K., Miller, P.I., Swan, S.C., Grant, M.G., Bresnan, E., 2012. An adaptive approach to detect high-biomass algal blooms from EO chlorophyll-a data in support of harmful algal bloom monitoring. Remote Sens. Lett. 3, 101–110. https://doi.org/10.1080/01431161.2010.538089.

Siemering, B., Bresnan, E., Painter, S.C., Daniels, C.J., Inall, M., Davidson, K., 2016. Phytoplankton distribution in relation to environmental drivers on the North West European Shelf Sea. PLoS ONE 11, e0164482. https://doi.org/10.1371/journal.pone.0164482.

Sourisseau, M., Jegou, K., Lunven, M., Quere, J., Gohin, F., Bryere, P., 2016. Distribution and dynamics of two species of Dinophyceae producing high biomass blooms over the French Atlantic Shelf. Harmful Algae 53, 53–63. https://doi.org/10.1016/j.hal.2015.11.016.

Stumpf, R.P., Culver, M.E., Tester, P.A., Tomlinson, M., Kirkpatrick, G.J., Pederson, B.A., Truby, E., Ransibrahmanakul, V., Soracco, M., 2003. Monitoring *Karenia brevis* blooms in the Gulf of Mexico using satellite ocean color imagery and other data. Harmful Algae 2, 147–160.

Stumpf, R.P., Tomlinson, M.C., Calkins, J.A., Kirkpatrick, B., Fisher, K., Nierenberg, K., Currier, R., Wynne, T.T., 2009. Skill assessment for an operational algal bloom forecast system. J. Mar. Syst. 76, 151–161. https://doi.org/10.1016/j.jmarsys.2008.05.016.

Swan, S.C., Turner, A.D., Bresnan, E., Whyte, C., Paterson, R.F., McNeill, S., Mitchell, E., Davidson, K., 2018. *Dinophysis acuta* in Scottish coastal waters and its influence on diarrhetic shellfish toxin profiles. Toxins (Basel) 10, 399. https://doi.org/10.3390/toxins10100399.

Thiétart, R.A., Forgues, B., 1995. Chaos theory and organization. Organ. Sci.

Whyte, C., Swan, S., Davidson, K., 2014. Changing wind patterns linked to unusually high *Dinophysis* blooms around the Shetland Islands, Scotland. Harmful Algae 39, 365–373. https://doi.org/10.1016/j.hal.2014.09.006.

Wyatt, T., Zingone, A., 2014. Population dynamics of red tide dinoflagellates. Deep. Res. Part II Top. Stud. Oceanogr. 101, 231–236. https://doi.org/10.1016/j.dsr2.2013.09.021.